frontiers | Frontiers in Ecology and Evolution

TYPE Original Research
PUBLISHED 14 March 2023
DOI 10.3389/fevo.2023.1147335

OPEN ACCESS

EDITED BY
Peter David Roopnarine,
California Academy of Sciences,
United States

REVIEWED BY
Mao Luo,
Nanjing Institute of Geology and Paleontology (CAS),
China

*CORRESPONDENCE
Yunfei Huang
✉ yfhuang@yangtzeu.edu.cn

SPECIALTY SECTION
This article was submitted to Paleontology,
a section of the journal
Frontiers in Ecology and Evolution

RECEIVED 18 January 2023
ACCEPTED 24 February 2023
PUBLISHED 14 March 2023

CITATION
Ji X, Huang Y, Sun X, Qiu X, Yang H, Tong J, Yi X and Tian L (2023) Ostracodal evolution during the Permian–Triassic transition at the Youping section of the Nanpanjiang Basin. *Front. Ecol. Evol.* 11:1147335. doi: 10.3389/fevo.2023.1147335

Ostracodal evolution during the Permian–Triassic transition at the Youping section of the Nanpanjiang Basin

Xia Ji[1], Yunfei Huang[1]*, Xin Sun[2], Xincheng Qiu[2], Hao Yang[2], Jinnan Tong[2], Xuefei Yi[1] and Li Tian[2]

[1]School of Geosciences, Yangtze University, Wuhan, China, [2]State Key Laboratory of Biogeology and Environmental Geology, China University of Geosciences, Wuhan, China

The Permian–Triassic mass extinction has been considered the largest bio-crisis of the Phanerozoic, with more than 90% of marine species extinct. Previous studies showed that ostracods suffered various extinction patterns in different localities and were relatively enriched in the lowermost Triassic shallow marine microbialites. Multiple hypotheses have been put forward to explore the reasons for this phenomenon. Abundant ostracod fossils were collected from the microbialite-bearing Youping section in the Nanpanjiang Basin. 45 species in 22 genera from Wujiaping Formation increased dramatically to 104 species in 33 genera from the microbialites of basal Luolou Formation. However, Ostracods from the Youping section suffered severe extinction during the second phase of the Permian–Triassic crisis, i.e., the earliest Triassic mass extinction (ETME), rather than the first phase, i.e., the latest Permian mass extinction (LPEM). In addition, the Sørenson coefficient has been used to examine the similarity of faunal associations among different sections of the Permian–Triassic transitional beds. There was no significant differences for ostracods between microbialites and non-microbialites sections based on similarity analysis. Thus, we proposed that "Shallow marine refuge" hypothesis could explain the high diversity and high abundance of ostracods of the Permian–Triassic transitional beds. Besides, ostracods showed remarkable geographical differentiation at both regional and global scales during the Permian–Triassic transitional beds and were presumably controlled by geographical isolation.

KEYWORDS

Permian–Triassic mass extinction, microbialites, ostracod, South China, faunal similarity

1. Introduction

The mass extinction at the Permian–Triassic transition was the largest biotic crisis in the Phanerozoic, resulting in the disappearance of more than 90% of marine species (Jablonski, 1994; Benton and Twitchett, 2003; Shen et al., 2011; Fan et al., 2020). Animals suffered either two-phased or single-phased mass extinction during the Permian–Triassic crisis (e.g., Song et al., 2013; Shen et al., 2019). The Lower Triassic carbonates are skeleton-poor worldwide but few shelly beds are dominated by disaster/opportunistic molluscs and small ostracods (Fraiser et al., 2005; Foster et al., 2019). Many studies have focused on the taxonomic distribution of ostracods (Crasquin et al., 2008; Forel et al., 2013a, 2015; Gliwa et al., 2021) and further explored the extinction, survival, and recovery patterns during the Permian–Triassic transition and its

aftermath (e.g., Crasquin and Forel, 2013; Forel et al., 2013a; Qiu et al., 2019).

In comparison with fossil records in various facies, ostracods enriched considerably in the Permian–Triassic boundary microbialites (PTBMs; Crasquin et al., 2008, 2010; Liu et al., 2010; Forel et al., 2013a, 2015). A few hypotheses were proposed to explain the high abundance and diversity of ostracods after the latest Permian mass extinction, i.e., the "microbialites refuge" hypothesis and the "shallow-water refuge" hypothesis (Forel et al., 2013a; Qiu et al., 2019). The "microbialites refuge" hypothesis considered Permian–Triassic microbialites as a refuge for ostracods (Forel et al., 2013a), however, the higher diversity and abundances of molluscan fossils in non-microbialites facies than in microbialites facies indicated the preferential preservation effect of transported fossils in microbialites (Foster et al., 2019). The abundant ostracods from non-microbialites sections Yangou and Aras Valley also challenge the "microbialites refuge" hypothesis but support the "shallow-water refuge" hypothesis (Qiu et al., 2019), which still needs more evidence.

In order to explore the extinction and survival patterns of the ostracod fauna during the Permian–Triassic transition, we investigated the ostracods distribution of the Youping section, i.e., a PTBMs bearing shallow marine carbonates continuous section, in the Nanpanjiang Basin of South China Block. Meanwhile, quantified faunal similarity calculation is employed to test the existing hypotheses on the blooming dynamics of ostracods in the PTBMs.

2. Geological setting

The South China Block, located at the eastern margin of the Paleo-Tethys Ocean during the Permian and Triassic periods, consisting of the Yangtze Platform, Zhejiang-Fujian-Guangdong clastic region and Nanpanjiang Basin (Figure 1; Tong and Yin, 2002; Yin et al., 2014). The Nanpanjiang Basin, which featured relatively deep water sediments, is mainly distributed in Guangxi Province and southern Guizhou Province (Enos et al., 2006). Several isolated carbonate platforms, including the Great Bank of Guizhou, Chongzuo, Pingguo, Debao, Jinxi and Luolou platforms, had developed in the Nanpanjiang Basin during the Late Permian to earliest Triassic (Figure 1; Lehrmann et al., 1998; Enos et al., 2006).

The Youping section is about 10 km north of Youping Town, Leye County, Guangxi Province, China. The succession, which has a thickness of 16.2 m, comprises the Upper Permian Wujiaping Formation and Lower Triassic Luolou Formation. The Wujiaping Formation was dominated by dark-grey thick-bedded bioclastic limestones, indicating a shallow platform environment (Figure 2). The basal Luolou Formation is composed of thick-bedded microbialites, overlied by thin-bedded to medium-bedded limestones and intercalated mudstones (Figure 2). The microbialites is about 8.2 m in thickness. The base of the microbialites of the Youping section was assigned to be Triassic in age, as for the presence of Triassic foraminifers and the carbon isotope excursion (Bagherpour et al., 2017).

3. Materials and methods

A total of 24 samples were collected from the Youping section, including five samples from the Wujiaping Formation, and 16 samples from the PTBMs of basal Luolou Formation, with three additional samples overlying the PTBMs (Figure 2). Three sample (YP-6, YP-11 and YP-14) from PTBMs yielded ostracods but were not analyzed to the species level. Bulk samples were finely crushed into tiny pieces of 1 cm^3 in the laboratory and then dissolved by acetic acid in a heated sand bath at a temperature of 70–80°C for an interval ranging from two days to three weeks. The undissolved sample remains were washed through 200 meshed sieves and dried. In total, 3,717 ostracod specimens have been obtained. Almost all specimens were

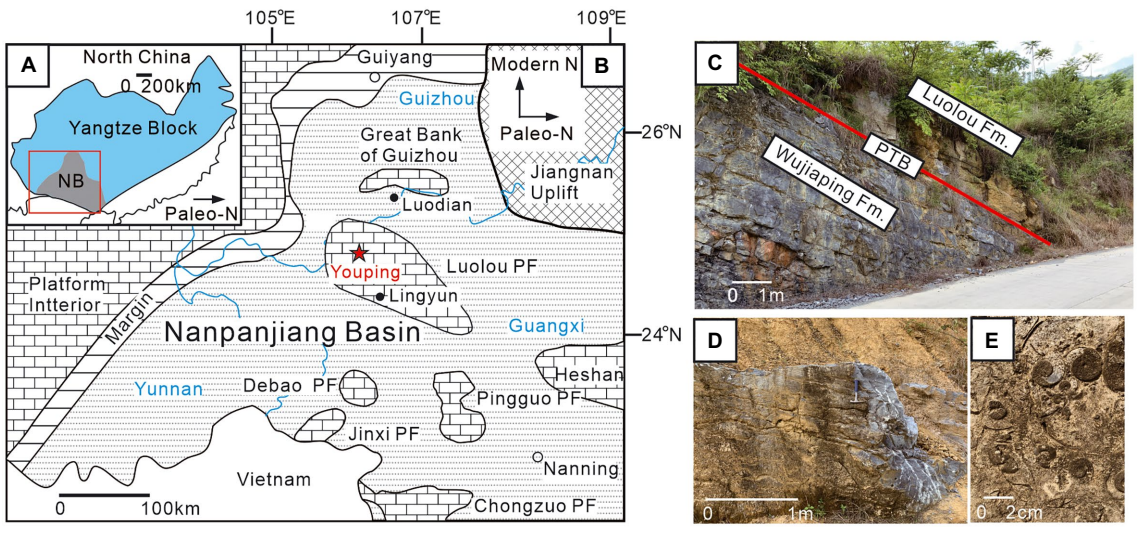

FIGURE 1
Paleogeographic map of the Nanpanjiang Basin and outcrop photos of the Youping section. **(A)** Paleogeographic map of South China Block (modified after Lehrmann et al., 1998); **(B)** locality of the Youping section (red star); **(C)** the Permian–Triassic boundary (PTB, red lined) at the Youping section; **(D)** microbialites of the basal Louluo Formation; **(E)** shell bed within the upperpart of microbialites. Fm, Formation; PF, Platform.

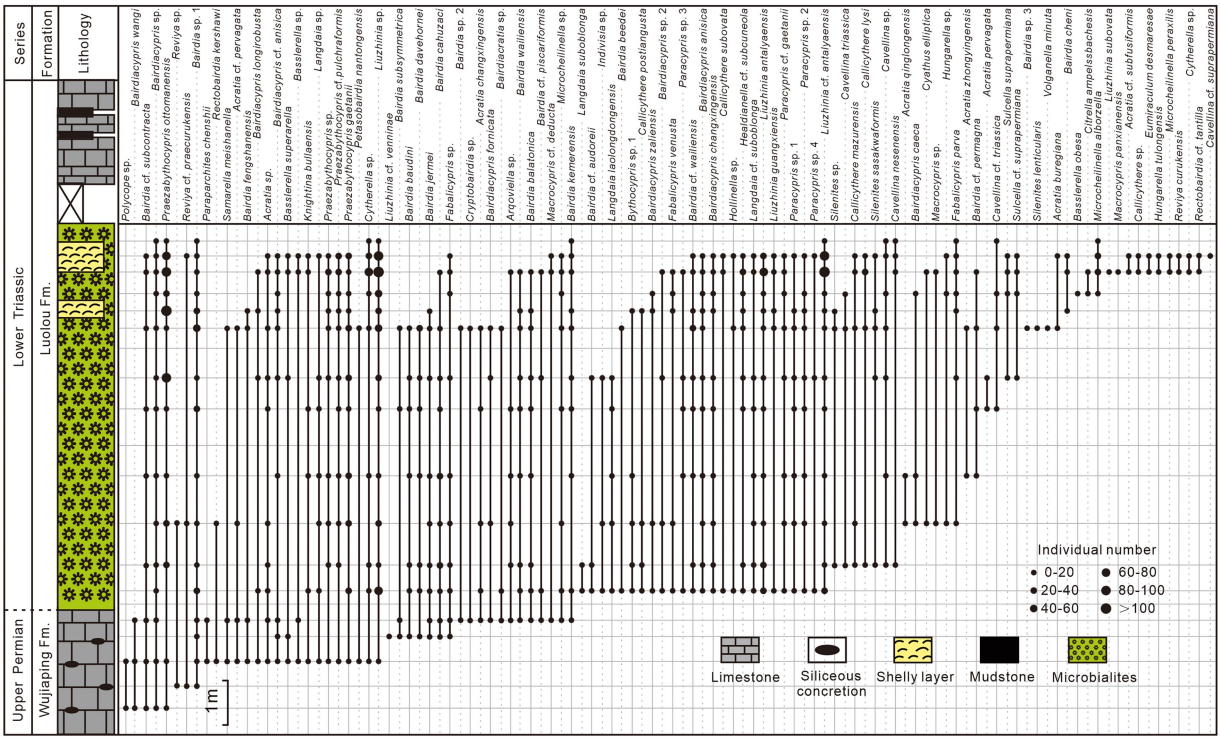

FIGURE 2
Distribution of ostracods fossils at the Youping section.

double-lobed shells with smooth shell surfaces (Figures 3–5). All fossil specimens were photographed by VEGA3 TESCAN scanning electron microscope and housed at the School of Geosciences, Yangtze University, Wuhan City, Hubei Province.

The individual numbers, species and genera richness, and relative abundances at the genus and family levels were used to reflect the ostracodal diversity changes in this study (Figure 6). Cluster analysis was carried out to recognize different ostracod communities through the Paleontological Statistics Software Package (PAST version 4.03) (Hammer et al., 2001). The Bray-Curtis parameter was selected to compare the similarities between ostracod fossils from different samples. Four communities were recognized (Figure 7). Besides, Shannon index, Evenness index and Dominance index were taken as diversity indexes (Figure 7). In addition, rarefaction analysis was taken out to test the sampling efficiency of various communities (Figure 7). When the rarefaction curve becomes flat and shows a typical banana shape, the sample could be considered sufficient (Hammer et al., 2001). The rarefaction curves for Community 2 and 3 indicate sufficient sampling, while the steep rarefaction curves for Community 1 and 4 indicate insufficient sampling (Figure 8).

We also established a small database on the ostracodal taxonomic compositions from several well-studied Permian–Triassic boundary (PTB) sections (Table 1), including Bulla and Bálvány-North sections of the western Paleotethys realm (Crasquin et al., 2008; Forel et al., 2013a,b), as well as Aras Valley, Çürük Dağ, and Elikah River sections of Cimmerian terranes (Crasquin et al., 2004a,b; Forel et al., 2015; Gliwa et al., 2021), and Meishan, Yangou, Panjiazhuang, Chongyang, Laolongdong, Dajiang, Zuodeng and Youping sections of the eastern Paleotethys realm (Crasquin et al., 2010; Liu et al., 2010; Forel, 2012; Qiu et al., 2019; Wan et al., 2019; Wan, 2021).

The fauna similarity between different sections is expressed by the Sørenson coefficient (also known as the Dice coefficient). Sørenson coefficient could be calculated by the following formula:

$$QS = 2c / (a + b)$$

Where QS is the Sørenson coefficient, a and b are the numbers of the genera at each section, and c means the number of shared genera between different sections (Sørenson, 1948; Jost et al., 2011). The Sørenson coefficient is positively correlated with the numbers of shared genera (Table 2). The QS value has been widely applied to analyze fauna similarities between different sites or communities, such as radiolarians, ammonites, and bivalves (e.g., Zacaï et al., 2016; Suárez-Mozo et al., 2021; Xiao et al., in press). The similarity of ostracod faunas at the genus level between different sections has been recovered (Table 2; Figure 9). The values of similarity are divided into three levels: low similarity (QS < 0.3), moderate similarity (QS between 0.3 and 0.5), and high similarity (QS > 0.5).

4. Results

The individual numbers of ostracods from each sample within the microbialites are usually over 130, significantly higher than those of the Wujiaping Formation (Figure 6). The specimen abundance increased abruptly from 48 to 322, followed by a peak of 763 in the

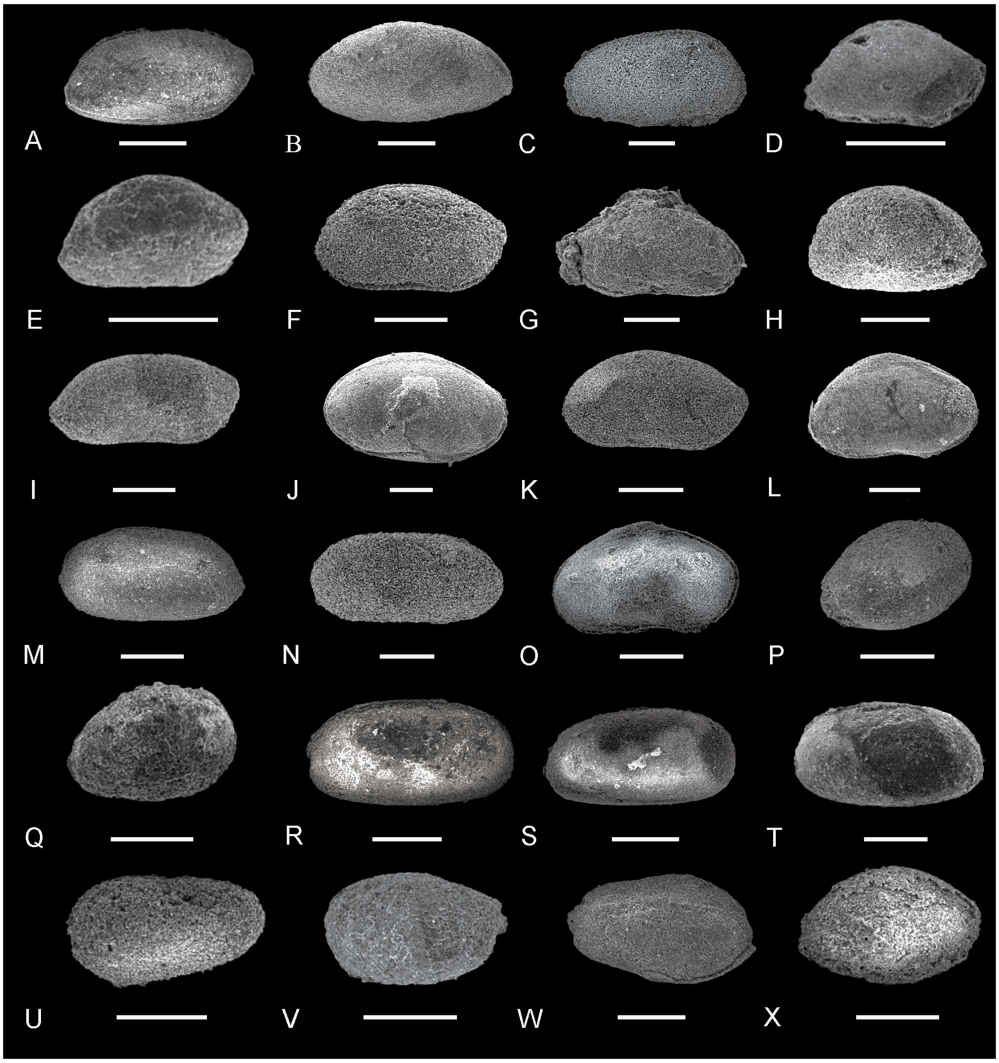

FIGURE 3
Ostracods from the Youping Section (I). **(A)** *Acratia cf. subfusiformis* Wang, right lateral view, sample YP-18; **(B)**, *Acratia* sp., left lateral view, sample YP-3; **(C)**, *Aqoviella* sp., right lateral view, sample YP-9; **(D)** *Bairdia beedei* Ulrich and Bassler, right lateral view, sample YP-7; **(E,F)** *Bairdia cahuzaci* Forel, right lateral view, sample YP-7 and YP-8; **(G)** *Bairdia davehornei* Forel, right lateral view, sample YP-7; **(H)** *Bairdia jermei* Forel, left lateral view, sample YP-5; **(I)** *Bairdia kemerensis* Crasquin-Soleau, right lateral view, sample YP-15; **(J)** *Bairdia subsymmetrica* Shi, left lateral view, sample YP-4; **(K)** *Bairdia wailiensis* Crasquin-Soleau, right lateral view, sample YP-8; **(L)** *Bairdiacratia* sp., right lateral view, sample YP-5; **(M,N)** *Bairdiacypris changxingensis* Shi, right lateral view, sample YP-18; **(O)** *Bairdiacypris fornicata* Shi, right lateral view, sample YP-5; **(P,Q)** *Basslerella superarella* Crasquin, right lateral view, sample YP-18; **(R,S)** *Callicythere lysi* Crasquin-Soleau, right lateral view, sample YP-18; **(T)** *Callicythere mazurensis* Styk, left lateral view, sample YP-18; **(U)** *Callicythere postiangusta* Wei, left lateral view, sample YP-8; **(V,W)** *Cavellina nesenensis* Crasquin, **V**: left lateral view; **W**: right lateral view, sample YP-18; **(X)** *Citrella ampelssbachensis* Kozur and Bolz, right lateral view, sample YP-17. Scale bars=200μm.

upper PTBMs (sample YP-18) (Figure 6). A distinct decrease, from 587 to 17, of specimen richness occurred at the top of PTBMs. No ostracods were found in sediments overlying the microbialites (Figure 6).

Both species and genus richness showed a fluctuated increasing trend from the Wujiaping Formation to the basal Luolou Formation (Figure 6). Only four species went extinct at the formation boundary, whilst all genera survived into the PTBMs (Figure 2). There was no obvious diversity change in samples before and above the PTB boundary. Significant diversity reduction, from 55 species of 22 genera to 12 species of eight genera, was not occurring until the upper PTBMs (sample YP-20; Figure 6).

Genus *Bairdia* was one of the most abundant genera, with the individual proportion ranging from 3.33% (sample YP-17) to 66.67% (sample YP-4), however, the individual proportion of genus *Bairdia* decreased gradually at the PTBMs of the Youping section (Figure 6). Genus *Paracypris* and *Liuzhinia* increased in abundance significantly at the formational contact, with *Paracypris* increased from 4.17% at YP-3 to 13.95% at YP-13 and *Liuzhinia* from 4.17% at YP-3 to 16.67% at YP-20, whilst the individual proportion of genus *Bairdiacypris* remaining stable (Figure 6). Genus *Cavellina* showed up with the development of PTBMs, occupying a certain proportion ranging from 2.7% at YP-10 to a high of 25% at YP-20 (Figure 6). At the family level, Bairdiidae dominated all samples, with proportions commonly higher than 50% (Figure 6). Family Cavellinidae and Bythocyprididae were new in the PTBMs, with the lowest value of 2.78% (sample YP-8) and the highest value of 25% (sample YP-20), while the relative abundances of Family

10.3389/fevo.2023.1147335

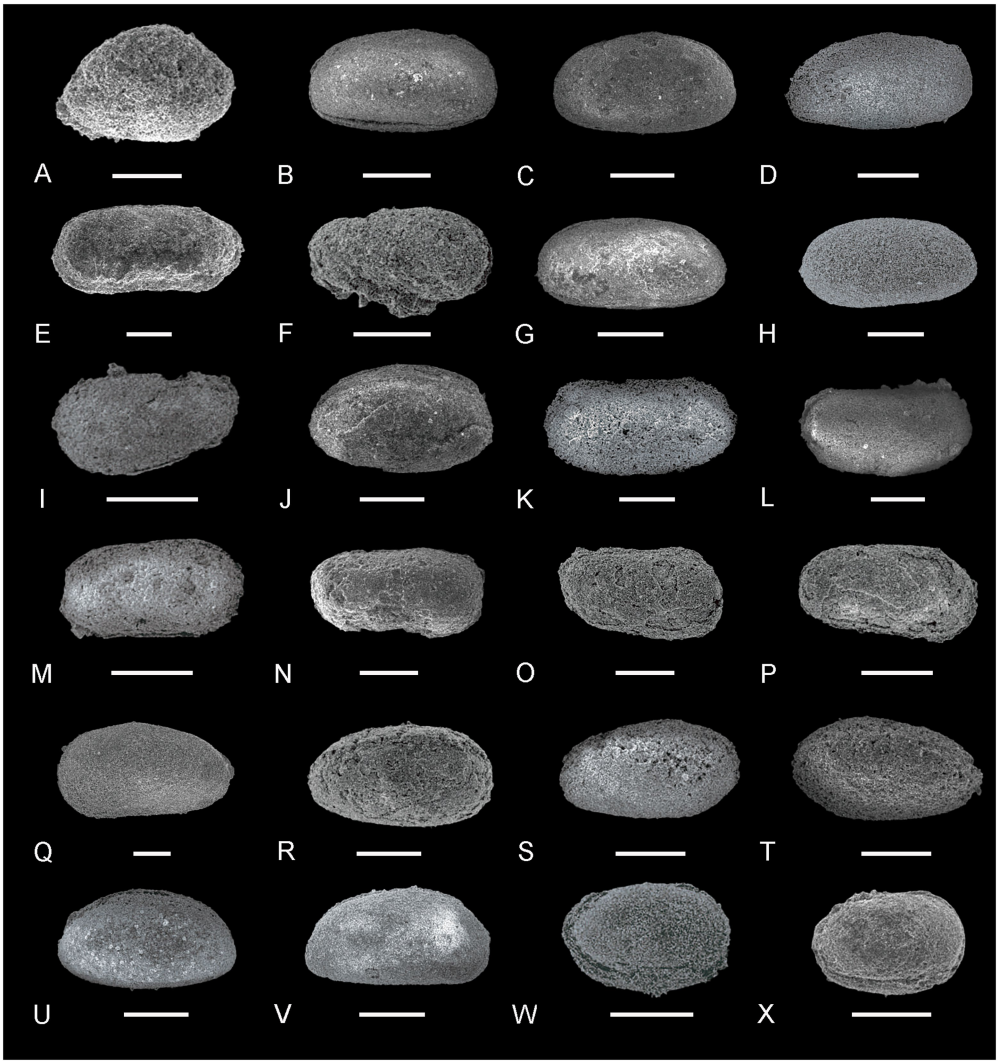

FIGURE 4
Ostracods from the Youping Section (II). **(A)** *Cryptobairdia* sp., right lateral view, sample YP-5; **(B,C)** *Cytherella* sp., right lateral view, sample YP-18; **(D,E)** *Fabalicypris parva* Wang, **D**: right lateral view, sample YP-18; **E**: left lateral view, sample YP-20; **(F)** *Fabalicypris venusta* Guan, right lateral view, sample YP-7; **(G,H)** *Healdianella cf. subcuneola* Posner, left lateral view, sample YP-18; **(I)** *Hollinella* sp., left lateral view, sample YP-7; **(J)** *Hungarella tulongnsis* Crasquin, right lateral view, sample YP-18; **(K,L)** *Indivisia* sp., right lateral view, sample YP-13; **(M,N)** *Langdaia laolongdongensis* Crasquin-Soleau and Kershaw, right lateral view, sample YP-7; **(O,P)** *Langdaia cf. suboblonga* Wang, right lateral view, sample YP-7; **(Q,R)** *Liuzhinia antalyaensis* Crasquin-Soleau, **Q**: left lateral view, sample YP-16; **R**: right lateral view, sample YP-7; **(S,T)** *Liuzhinia guangxiensis* Crasquin-Soleau, **S**: right lateral view, sample YP-19; **T**: left lateral view, sample YP-18; **(U)** *Macrocypris cf. deducta* Zalanyi, left lateral view, sample YP-19; **(V)** *Macrocypris panxianensis* Wang, right lateral view, sample YP-18; **(W,X)** *Microcheilinella alborzella* Forel, right lateral view, sample YP-19. Scale bars=200μm.

Paraparchitidae and Acratiidae decreased sharply in the upper part of PTBMs (Figure 6).

Four communities have been recognized through cluster analysis (Figure 7). Community 1 consist of samples YP-1 to YP-5, corresponding to the limestone of the Wujiaping Formation, and is characterized by abundant *Bairdia* (38.89%) and *Reviya* (22.22%). Community 2 contains samples from YP-7 to YP-17 in the PTBMs and was dominated by the genus *Bairdia* (23.10%), *Liuzhinia* (22.12%) and *Praezabythocypris* (19.49%). Samples YP-18 and YP-19 in the PTBMs are clustered as Community 3, which was dominated by the genus *Liuzhinia* (37.04%) and *Praezabythocypris* (17.04%). Sample YP-20 from the uppermost part of PTBMs is assigned to Community 4, which was featured by the genus *Bairdia* (23.53%), *Cavellina* (17.65%) and *Praezabythocypris* (17.65%). Diversity indexes of four communities showed significant variations. The Shannon index decreased gradually, but the Dominance index increased gradually from Community 1 to Community 4, while the Evenness index declined from communities 1 to 3, followed by a rebound in community 4 (Figure 7).

5. Discussion

5.1. Extinction pattern of ostracods during the Permian–Triassic

The diversity of the ostracods at the Youping section increased from the uppermost Permian Wujiaping Formation to the Lower

10.3389/fevo.2023.1147335

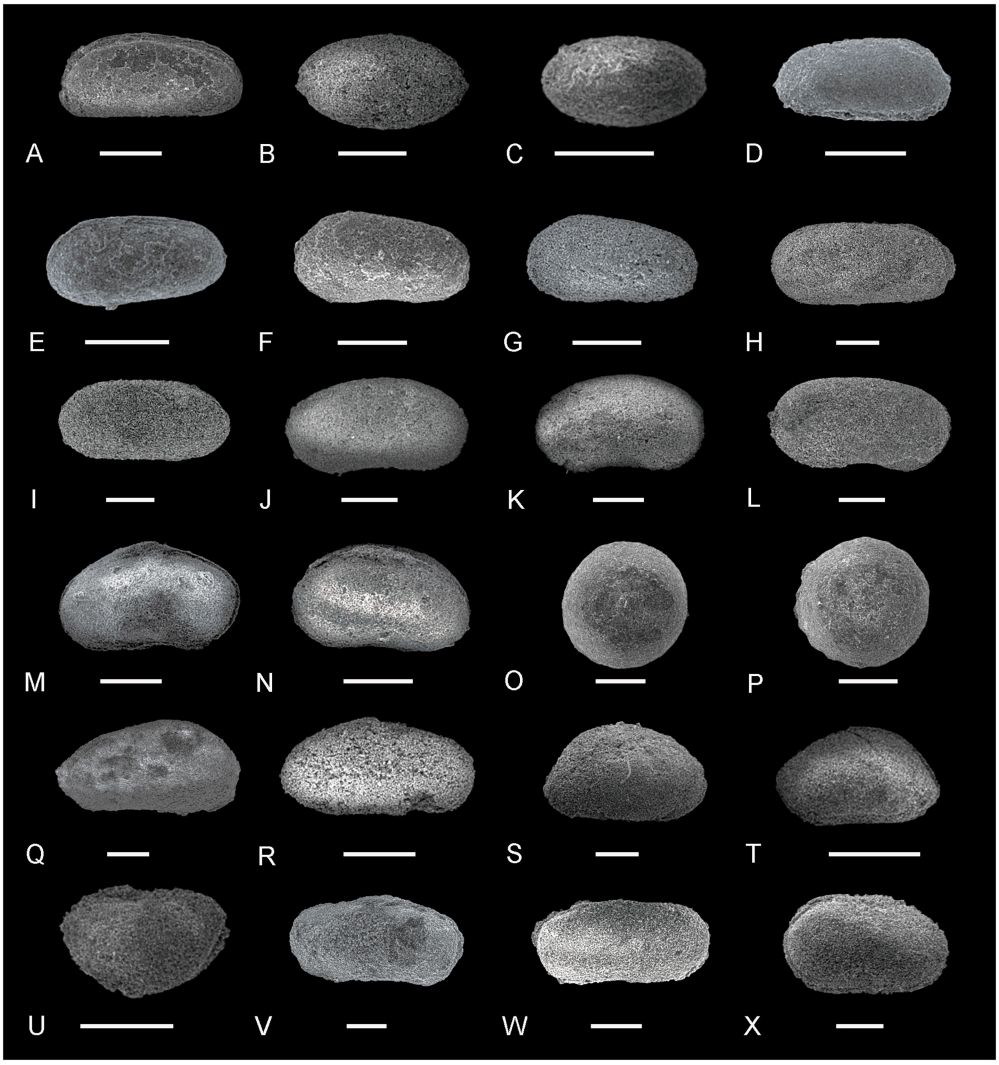

FIGURE 5
Ostracods from the Youping Section (III). **(A)** *Microcheilinella peraxilis* Shi, left lateral view, sample YP-18; **(B,C)** *Microcheilinella* sp., right lateral view, sample YP-7 and YP-9; **(D,E)** *Paracypris gaetanii* Crasquin-Soleau, **D**: right lateral view, sample YP-19; **E**: left lateral view, sample YP-19; **(F,G)** *Paracypris* sp. 2, left lateral view, sample YP-9; **(H,I)** *Paracypris* sp. 1, **H**: left lateral view, sample YP-16; **I**: right lateral, sample YP-16; **(J–L)** *Praezabythocypris ottomanensis* Crasquin-Soleau, right lateral view, **J,K**: sample YP-13; **L**: sample YP-16; **(M,N)** *Prazathocypris cf. pulchraformis* Forel, **M**: right lateral view, sample YP-19; **N**: left lateral view, sample YP-19; **(O,P)** *Polycope* sp., right lateral view, sample YP-3; **(Q)** *Rectobairdia cf. tantilla* Kummerow, right lateral view, sample YP-18; **(R,S)** *Silenites sasakwaformis* Shi, right lateral view, sample YP-13 and YP-15; **(T)** *Silenites lenticularis* Knight, right lateral view, sample YP-15; **(U)** *Smarella meishanella* Forel, left lateral view, sample YP-15; **(V,W)** *Sulce suprapermianana* Kozur, right lateral view, sample YP-17 and YP-19; **(X)** *Volganella minuta* Wang, left lateral view, sample YP-15. Scale bars=200μm.

Triassic Luolou Formation, rather a rapid decrease as shown at the GSSP Meishan and a few other sections. At the Permian–Triassic boundary GSSP Meishan section, ostracodal diversity reduced from 95 species in 43 genera of the latest Permian to two species in two genera from bed 27 (Crasquin et al., 2010; Table 1). At the Bulla section of Italy (Table 1), ostracodal diversity reduced from 54 species in 25 genera to nine species in eight genera from the conodont *Hindeodus praeparvus* zone (Crasquin et al., 2008). A similar rapid decrease of ostracods from the uppermost Permian to the Permain-Triassic transitional beds (PTTB) (Table 1) was also reported at the Dajiang section of South China (Forel, 2012), Elikah River section of north Iran (Forel et al., 2015), Bálvány North section of Hungary (Forel et al., 2013a), and Çürük Dağ section of Turkey (Crasquin et al., 2004a,b). However, at the Youping section of this study, 45 species in 22 genera of ostracod fauna occurred in the uppermost Permian limestone and increased to 104 species in 33 genera from the PTBMs (Figure 2; Table 1). Similarly, ostracodal diversity increases from Permian bioclastic limestone to the PTTB also have been observed at several sections of shallow carbonate facies, e.g., the Aras Valley (Gliwa et al., 2021), Zuodeng (Wan et al., 2019), and Panjiazhang sections (Wan, 2021; Table 1).

Ostracod disappeared at the top of the PTBMs at the Youping section, potentially corresponding to the ETME, i.e., the second extinction phase of the Permian–Triassic crisis in Song et al. (2013). The ostracodal taxonomic diversity of many microbialite-bearing shallow carbonate sections, e.g., Youping, Panjiazhuang, and Zuodeng, suffered a critical drop along with the demises of microbialites (Table 1). No ostracod taxa was observed in samples YP-21 to YP-24 at the Youping section, and only two species in sample Zd-44 survived in the thin-bedded limestone overlying PTBMs at the Zuodeng

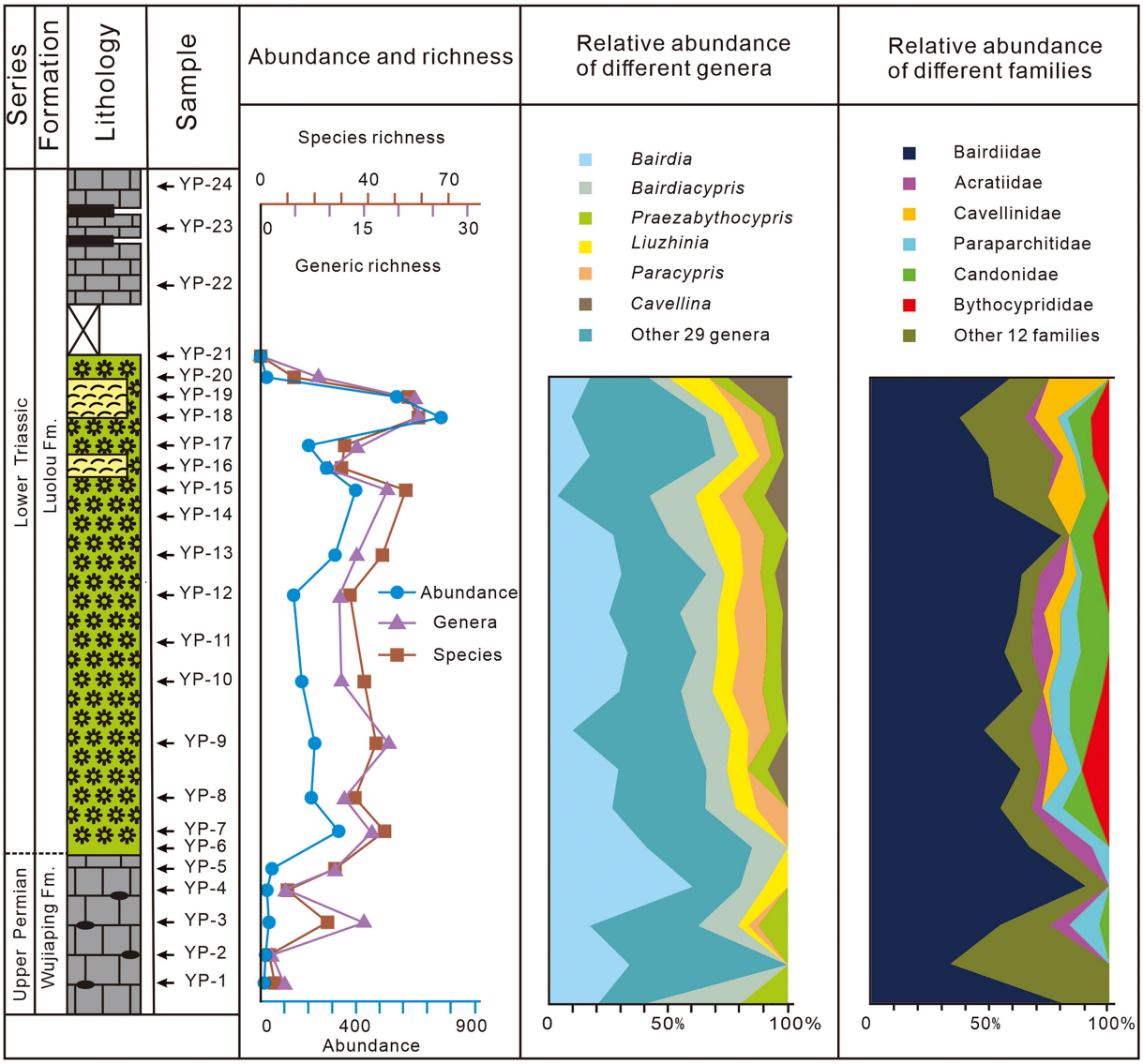

FIGURE 6
Temporal variations of the ostracodal diversity, abundances and compositions throughout the Youping section.

section (Wan et al., 2019). The Panjiazhuang section also shows a decreasing trend from 68 species in 17 genera in beds two and three to 27 species in seven genera in bed 4 (Wan, 2021). Similarly, ostracod diversity of the Aras Valley section reduced sharply from 51 species in 19 genera during the conodont *Hindeodus praeparvus* zone to five species in three genera from the conodont *Isarcicella staeschei* zone (Gliwa et al., 2021).

A set of microbialites usually formed on the carbonate platforms in the aftermath of the EPME (e.g., Lehrmann et al., 1998; Wang et al., 2005; Kershaw et al., 2007, 2012; Tian et al., 2019; Foster et al., 2020). Studies on several microbialite-bearing sections, including Dajiang, Taiping and Pojue sections, suggest that the PTB is at the base of microbialites, for the first occurrence of *Hindeodus parvus* (Jiang et al., 2014; Wang et al., 2016; Xiao et al., 2018; Chen et al., 2019). Although the precise age of the terminal PTBMs is unsure, the high-resolution conodont biostratigraphic zonation studies of Dajiang and Cili sections show the first occurrence of *Isarcicella isarcica* from the thin-bedded limestone overlying the PTBMs (Jiang et al., 2014; Wang et al., 2016), correlating to the second phase of the Permian–Triassic crisis, i.e., Earliest Triassic mass extinction (ETME; Song et al., 2013). Thus, the base and top of the Youping PTBMs are equivalent to the LPME and ETME horizons, respectively. Song et al. (2013) constrained the earliest Triassic mass extinction (ETME) to the *Isarcicella staeschei* zone. However, the Youping section shows that the ETME occurred at the top of the microbialites, which corresponds to the upper part of the *Hindeodus parvus* zone (Bagherpour et al., 2017), implying a potential earlier ETME at Youping.

5.2. Biogeographic controls on the ostracods during the Permian–Triassic transition

The "microbial-related refuge" hypothesis was proposed to explain the extremely high abundance and diversity of PTBMs (Forel et al., 2013b). Indeed, extremely high ostracodal diversity occurred at the

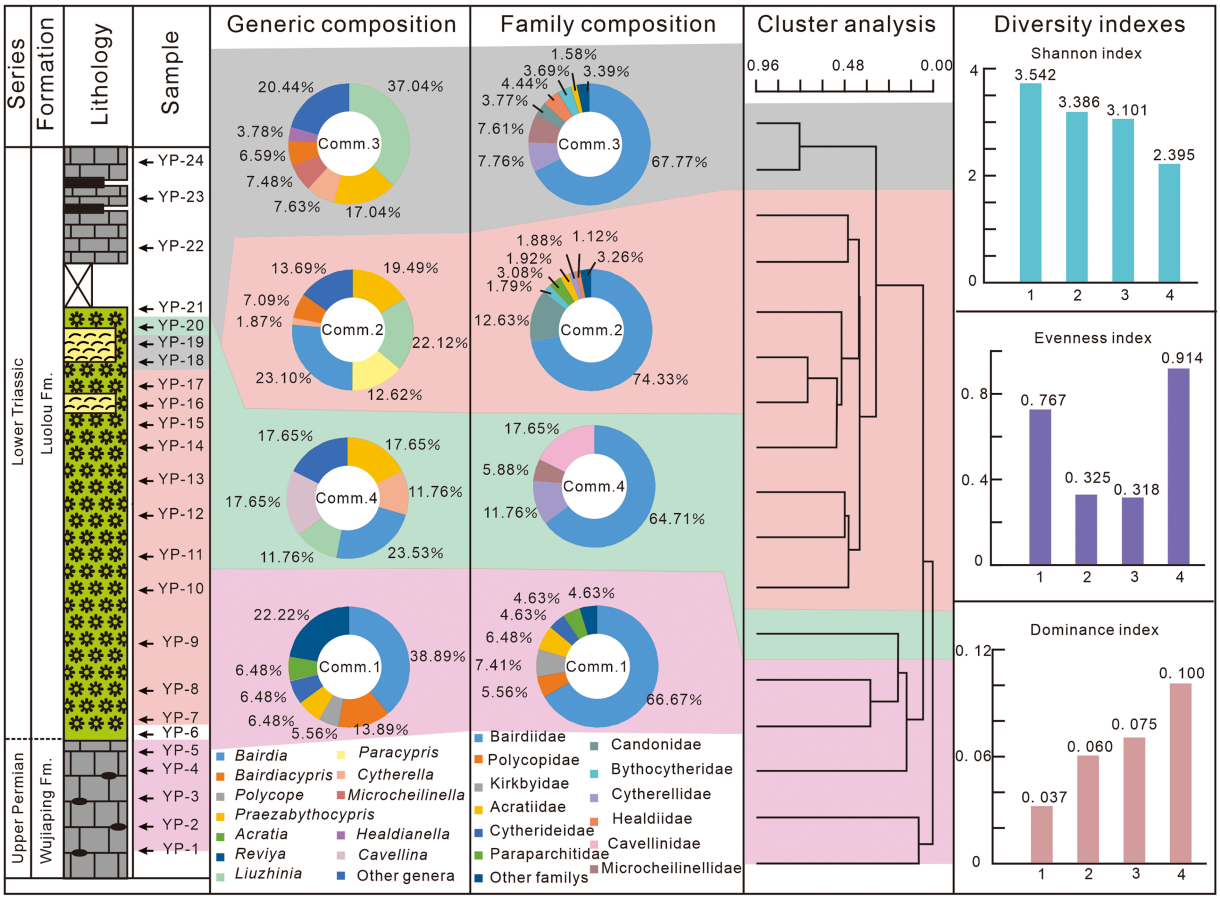

FIGURE 7
Ostracod communities based on cluster analysis, and their diversity indexes from the Youping section. Comm: Community.

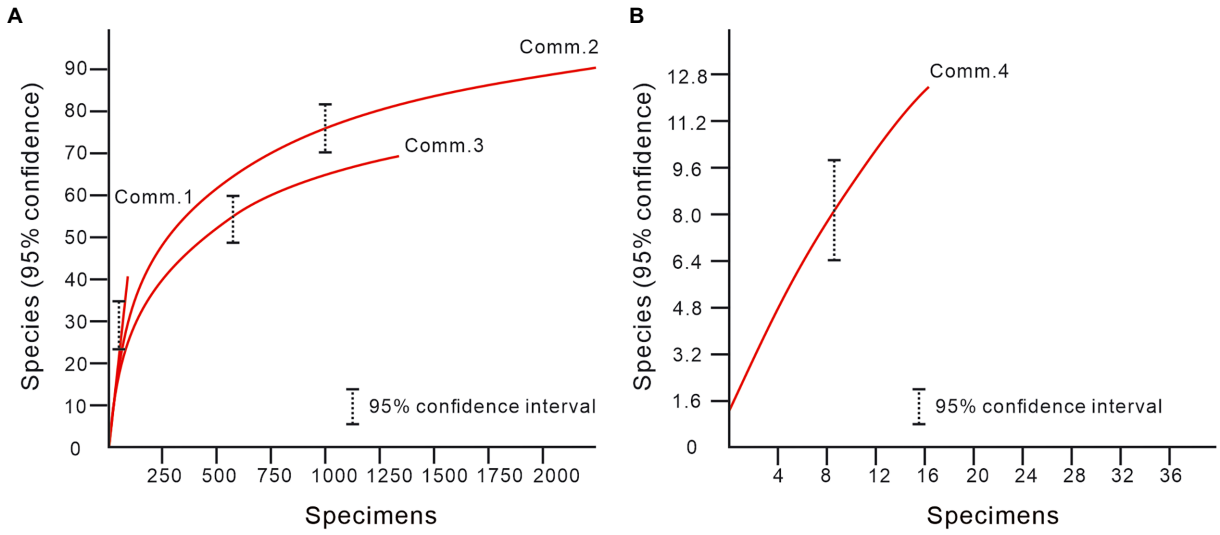

FIGURE 8
Rarefaction curves for four ostracod communities of the Youping section. Comm: Community.

Youping PTBMs (this study), the same as the circumstances at Aras Valley (Gliwa et al., 2021), Panjiazhang (Wan, 2021), Elikah River (Forel et al., 2015), Bálvány-North (Forel et al., 2013a), and Zuodeng sections (Wan et al., 2019). However, only moderate ostracodal diversity at the genus level has been seen in the PTBMs of Laolongdong (Crasquin and Kershaw, 2005), Chongyang (Liu et al., 2010), Dajiang

TABLE 1 Taxonomic diversity of ostracods from different sections during the Permian–Triassic.

Palaeogeographical facies	Section name	Pre-LPME	PTTB	Post-ETME	References
Non-microbialite shallow carbonate facies	Aras Valley	9 species of 8 genera	51 species of 19 genera	5 species of 3 genera	Gliwa et al. (2021)
	Yangou	*	33 speices of 8 genera	3 species of 2 genera	Qiu et al. (2019)
	Bulla	54 species of 25 genera	9 species of 8 genera	8 species of 6 genera	Crasquin et al. (2008)
Microbialite-bearing shallow carbonate facies	Youping	45 species of 22 genera	104 species of 33 genera	0	This study
	Panjiazhuang	22 species of 8 genera	68 species of 16 genera	27 species of 7 genera	Wan (2021)
	Zuodeng	25 species of 12 genera	47 species of 12 genera	2 species of 2 genera	Wan et al. (2019)
	Elikah River	61 species of 32 genera	33 species of 20 genera	*	Forel et al. (2015)
	Bálvány-North	54 species of 16 genera	36 species of 15 genera	*	Forel et al. (2013a,b)
	Laolongdong	*	14 species of 8 genera	*	Crasquin and Kershaw (2005)
	Chongyang	20 species of 6 genera	14 species of 7 genera	*	Liu et al. (2010)
	Dajiang	82 species of 25 genera	30 species of 7 genera	*	Forel (2012)
	Çürük Dağ	28 species of 19 genera	12 species of 6 genera	*	Crasquin et al. (2004a,b)
	Pojue	50 species of 13 genera	21 species of 6 genera	*	Wan (2021)
	Zhaixia	*	31 species of 7 genera	0	Wan (2021)
Slope and deep-sea facies	Meishan	95 species of 43 genera	2 species of 2 genera	3 species of 3 genera	Crasquin et al. (2010)

LPME, Latest Permian mass extinction; PTTB, Permian–Triassic transitional bed; ETME, Earliest Triassic mass extinction. *means no data.

TABLE 2 Sørenson coefficient values between each two sections during the Permian–Triassic transitional beds.

Sections name	YP	MS	BU	AV	YG	ZD	PJ	ZX	PJZ	CY	LLD	DJ	CD	ER	BN
YP	*	0.11	0.29	0.58	0.39	0.53	0.26	0.35	0.49	0.30	0.39	0.30	0.26	0.60	0.50
MS	0.11	*	0.20	0.10	0.20	0.14	0.25	0.22	0.11	0.22	0.20	0.22	0.25	0.09	0.00
BU	0.29	0.20	*	0.30	0.50	0.40	0.29	0.40	0.33	0.27	0.38	0.27	0.29	0.29	0.35
AV	0.58	0.10	0.30	*	0.44	0.52	0.32	0.38	0.51	0.31	0.37	0.38	0.40	0.51	0.53
YG	0.39	0.20	0.50	0.44	*	0.50	0.71	0.67	0.50	0.53	0.75	0.53	0.43	0.50	0.35
ZD	0.53	0.14	0.40	0.52	0.50	*	0.44	0.53	0.64	0.42	0.40	0.42	0.33	0.44	0.44
PJ	0.26	0.25	0.29	0.32	0.71	0.44	*	0.77	0.45	0.62	0.57	0.77	0.50	0.38	0.19
ZX	0.35	0.22	0.40	0.38	0.67	0.53	0.77	*	0.61	0.71	0.53	0.71	0.46	0.52	0.27
PJZ	0.49	0.11	0.33	0.51	0.50	0.64	0.45	0.61	*	0.43	0.42	0.43	0.27	0.56	0.39
CY	0.30	0.22	0.27	0.31	0.53	0.42	0.62	0.71	0.43	*	0.53	0.43	0.31	0.37	0.18
LLD	0.39	0.20	0.38	0.37	0.75	0.40	0.57	0.53	0.42	0.53	*	0.53	0.29	0.43	0.35
DJ	0.30	0.22	0.27	0.38	0.53	0.42	0.77	0.71	0.43	0.43	0.53	*	0.46	0.44	0.27
CD	0.26	0.25	0.29	0.40	0.43	0.33	0.50	0.46	0.27	0.31	0.29	0.46	*	0.31	0.29
ER	0.60	0.09	0.29	0.51	0.50	0.44	0.38	0.52	0.56	0.37	0.43	0.44	0.31	*	0.46
BN	0.50	0.00	0.35	0.53	0.35	0.44	0.19	0.27	0.39	0.18	0.35	0.27	0.29	0.46	*

YP Youping section; MS Meishan section; BU Bulla section; AV Aras Valley section; YG Yangou section; ZD Zuodeng section; PJ Pojue section; ZX Zhaixia section; PJZ Panjiazhuang section; CY Chongyang section; LLD Laolongdong section; DJ Dajiang section; CD Çürük Dağ; ER Elikah River section; BN Bálvány-North section. *means no data.

(Forel, 2012), and Çürük Dağ sections (Crasquin et al., 2004a,b), less diverse than the non-PTBMs bearing Yangou and Aras valley sections (Qiu et al., 2019; Gliwa et al., 2021), mismatching the "microbial related refuge" hypothesis.

Furthermore, the "microbial related refuge" hypothesis is also denied by the ostracodal faunal similarity analyses. Ostracodal fauna of PTBMs bearing sections show varied similarities, from low to high (Figure 9). Only moderate similarities were recorded among the sections of isolated platforms, i.e., Dajiang (Forel, 2012), Zuodeng (Wan et al., 2019), Pojue (Wan, 2021) and Youping sections, with Laolongdong (Crasquin and Kershaw, 2005), Chongyang (Liu et al., 2010) and Zhaixia (Wan, 2021) sections of the Yangtze Platform, albeit PTBMs occurred at all of them, implying no significant microbial related facies control. The highest similarities occurred at the Yangtze Platform sections, including the PTBMs bearing Laolongdong (Crasquin and Kershaw, 2005), Chongyang (Liu et al.,

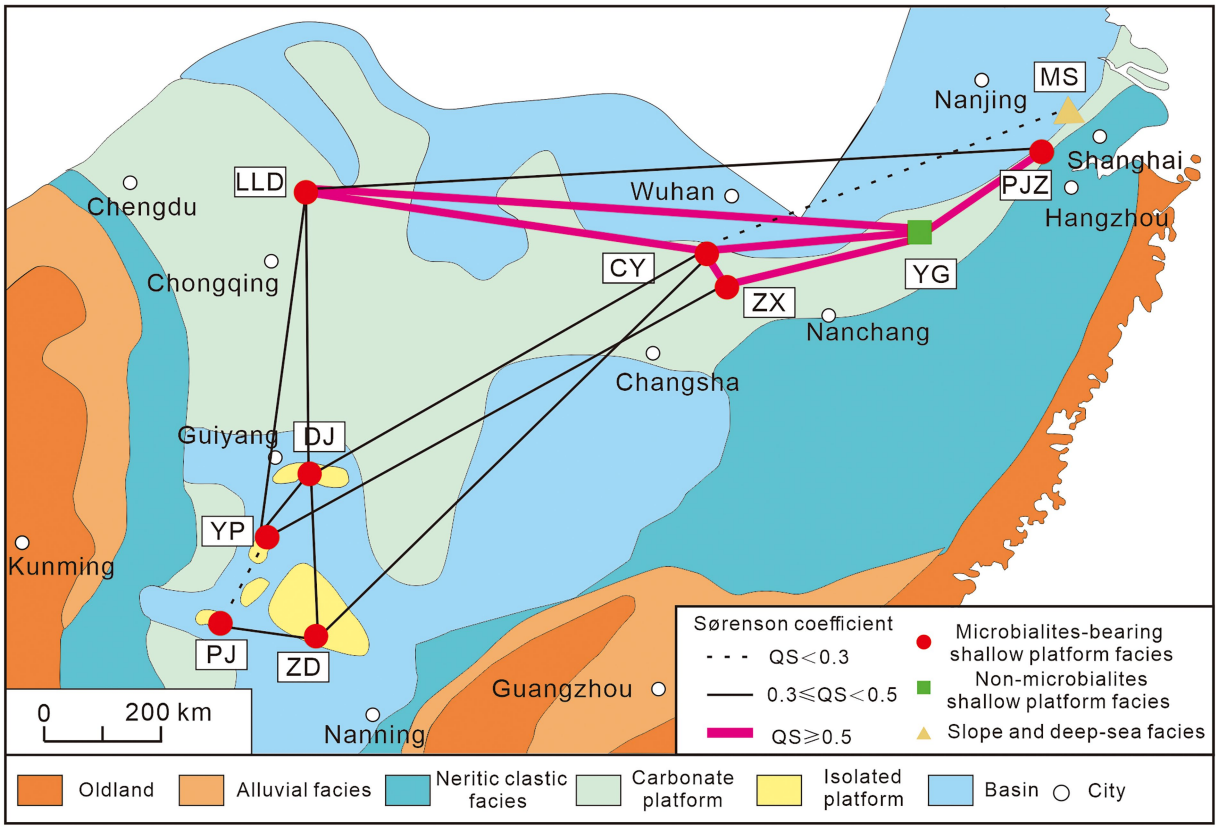

FIGURE 9
Similarities of ostracod fauna among different sections during the Permian–Triassic transitional beds. Paleogeography map of the South China modified after Yin et al. (2014). YP Youping section; ZD Zuodeng section; DJ Dajiang section; PJ Pojue section; LLD Laolongdong section; CY Chongyang section; ZX Zhaixia section; YG Yangou section; PJZ Panjiazhuang section; MS Meishan section.

2010), Zhaixia (Wan, 2021), Panjiazhuang (Wan, 2021) and the non-PTBMs bearing Yangou section, somewhat supporting the "shallow marine refuge" hypothesis (Qiu et al., 2019). In addition, moderate to high fauna similarities were shown between Bulla (Crasquin et al., 2008) and Bálvány-North (Forel et al., 2013a) in western Paleotethys with Aras valley (Gliwa et al., 2021) and Elikah River (Forel et al., 2015) in Cimmerian terranes (Table 2), indicating weak geographic isolation.

Increases of the cosmopolitan taxa in the post mass extinction, both in the marine invertebrates and terrestrial tetrapods, were documented (Button et al., 2017; Dai and Song, 2020; Zhang et al., 2022), so as the ostracods. Dai and Song (2020) proposed three models, i.e., (a) selective extinction among endemic taxa, (b) endemics becoming cosmopolitans and (c) newly originated cosmopolitans, for the elevated cosmopolitanism across the Permian–Triassic extinction event. In total, 50 ostracod genera had been discovered from the Permian–Triassic transitional beds mentioned above, at least nine of them were cosmopolitan. At the Youping section, the cosmopolitans contain *Callicythere, Hollinella, Fabalicypris, Langdaia, Acratia, Paracypris, Liuzhinia, Bairdia* and *Bairdiacypris*, among which *Acratia, Bairdia, Bairdiacypris, Langdaia, Paracypris* belong to Model b and *Callicythere, Fabalicypris, Hollinella* belong to Model c. Besides, the significant ostracod community transition from Community 1 to Community 2 around the Permian–Triassic boundary implies the dominance of several above-mentioned cosmopolitan genera, e.g., *Bairdia* and *Liuzhinia*. Although we do not have a specific biogeographic connectedness index of ostracods calculated as other studied groups, we hypotheses that the cosmopolitans elevation of ostracods might be less significant than ammonoids, anthozoan and bryozoan (Dai and Song, 2020; Zhang et al., 2022) during the Permian–Triassic mass extinction event, since ostracods are much more high-temperature and low oxygen tolerances than most other marine invertebrates (Song et al., 2014). Further biogeographic studies are needed to test our scenario to shed new light on deciphering the environmental dynamics of the extinction and survival of ostracods during the Permian–Triassic mass extinction.

6. Conclusion

This study presented the taxonomic distribution of ostracod fossils from the microbialite-bearing Youping section in the Nanpanjiang Basin: 45 species in 22 genera were found from the Wujiaping Formation while 104 species in 33 genera were identified from the microbialites of basal Luolou Formation. Ostracods disappeared at the top of microbialites, implying a potential earlier ETME at the Youping section. The similarity analysis did not show

significant differences between microbialites and non-microbialites sections, and does not support the "microbial related refuge" hypothesis, but supports the "shallow marine refuge" hypothesis. The biogeographic distribution of ostracods during the Permian–Triassic extinction requires further research to clarify the role of temperature and oxygen levels in the extinction event.

Data availability statement

The original contributions presented in the study are included in the article/supplementary material, further inquiries can be directed to the corresponding author.

Author contributions

YH, LT, JT, and XY designed the study. XQ, LT, HY, and XS collected rock samples in the field. XJ and XS analyzed the data. XJ, YH, and LT wrote the first draft of the manuscript, which received revision from all co-authors. All authors have contributed to the article and approved the submitted version.

Funding

This study was funded by the National Natural Science Foundation of China (grant number 42030513), and State Key Laboratory of Biogeology and Environmental Geology, China University of Geosciences (Grant numbers GBL22103 and GBL21708).

Conflict of interest

The authors declare that the research was conducted in the absence of any commercial or financial relationships that could be construed as a potential conflict of interest.

Publisher's note

All claims expressed in this article are solely those of the authors and do not necessarily represent those of their affiliated organizations, or those of the publisher, the editors and the reviewers. Any product that may be evaluated in this article, or claim that may be made by its manufacturer, is not guaranteed or endorsed by the publisher.

References

Bagherpour, B., Bucher, H., Baud, A., Brosse, M., Vennemann, T., Martini, R., et al. (2017). Onset, development, and cessation of basal early *Triassic microbialites* (BETM) in the Nanpanjiang pull-apart basin, South China block. *Gondwana Res.* 44, 178–204. doi: 10.1016/j.gr.2016.11.013

Benton, M. J., and Twitchett, R. J. (2003). How to kill (almost) all life: the end-Permian extinction event. *Trends Ecol. Evol.* 18, 358–365. doi: 10.1016/S0169-5347(03)00093-4

Button, D. J., Lloyd, G. T., Ezcurra, M. D., and Butler, R. J. (2017). Mass extinctions drove increased global faunal cosmopolitanism on the supercontinent Pangaea. *Nat. Commun.* 8:733. doi: 10.1038/s41467-017-00827-7

Chen, Y., Ye, Q., Jiang, H. S., Wignall, P. B., and Yuan, J. L. (2019). Conodonts and carbon isotopes during the Permian-Triassic transition on the Napo Platform, South China. *J. Earth Sci.* 30, 244–257. doi: 10.1007/s12583-018-0884-3

Crasquin, S., and Forel, M. B. (2013). Ostracods (Crustacea) through Permian-Triassic events. *Earth Sci. Rev.* 137, 52–64. doi: 10.1016/j.earscirev.2013.01.006

Crasquin, S., Forel, M. B., Feng, Q. L., Yuan, A. H., Baudin, F., and Collin, P. Y. (2010). Ostracods (Crustacea) through the Permian-Triassic boundary in South China: the Meishan stratotype (Zhejiang Province). *J. Syst. Palaeontol.* 8, 331–370. doi: 10.1080/14772011003784992

Crasquin, S., and Kershaw, S. (2005). Ostracod fauna from the Permian-Triassic boundary interval of South China (Huaying Mountains, eastern Sichuan Province): palaeoenvironment significance. *Palaeogeogr. Palaeoclimatol. Palaeoecol.* 217, 131–141. doi: 10.1016/j.palaeo.2004.11.027

Crasquin, S., Marcoux, J., Angiolini, L., Richoz, S., and Nicora, A. (2004a). Palaeocopida (Ostracoda) across the Permian-Triassic events: new data from southwestern Taurus(Turkey). *Micropalaeontology* 23, 67–76. doi: 10.1144/jm.23.1.67

Crasquin, S., Marcoux, J., Angiolini, L., Richoz, S., Nicora, A., Baud, A., et al. (2004b). A new ostracode fauna from the Permian-Triassic boundary in Turkey (Taurus, Antalya Nappes). *Micropaleontology* 50, 281–295. doi: 10.1661/0026-2803(2004)050[0281:ANOFFT]2.0.CO;2

Crasquin, S., Perri, M. C., Nicora, A., and Wever, P. D. (2008). Ostracods across the Permian-Triassic boundary in Western Tethys: the Bulla parastratotype (Southern Alps, Italy). *Riv. Ital. Paleontol. Stratigr.* 114, 233–262. doi: 10.13130/2039-4942/5900

Dai, X., and Song, H. J. (2020). Toward an understanding of cosmopolitanism in deep time: a case study of ammonoids from the middle Permian to the middle Triassic. *Paleobiology* 46, 533–549. doi: 10.1017/pab.2020.40

Enos, P., Lehrmann, D. J., Wei, J. Y., Yu, Y. Y., Xiao, J., Chaikin, D. H., et al. (2006). Triassic evolution of the Yangtze platform in Guizhou Province, Peoples Republic of China. *Geol. Soc. Am. Spec. Pap.* 417, 1–105. doi: 10.1130/2006.2417

Fan, J. X., Shen, S. Z., Erwin, D. H., Sadler, P. M., Macleod, N., Cheng, Q. M., et al. (2020). A high-resolution summary of Cambrian to early Triassic marine invertebrate biodiversity. *Science* 367, 272–277. doi: 10.1126/science.aax495

Forel, M. B. (2012). Ostracods (Crustacea) associated with microbialites across the Permian-Triassic boundary in Dajiang (Guizhou Province, South China). *Eur. J. Taxon.* 0, 1–34. doi: 10.5852/ejt.2012.19

Forel, M. B., Crasquin, S., Chitnarin, A., Angiolini, L., and Gaetani, M. (2015). Precocious sexual dimorphism and the Lilliput effect in Neo-Tethyan Ostracoda (Crustacea) through the Permian-Triassic boundary. *Palaeontology* 58, 409–454. doi: 10.1111/pala.12151

Forel, M. B., Crasquin, S., Hips, K., Kershaw, S., Collin, P. Y., and Haas, J. (2013a). Biodiversity evolution through the Permian-Triassic Boundary event: ostracods from the Bükk Mountains, Hungary. *Acta Palaeontol. Pol.* 58, 195–219. doi: 10.4202/app.2011.0126

Forel, M. B., Crasquin, S., Kershaw, S., and Collin, P. Y. (2013b). In the aftermath of the end-Permian extinction: microbialite refuge? *Terra Nova* 25, 137–143. doi: 10.1111/ter.12017

Foster, W. J., Heindel, K., Richoz, S., Gliwa, J., Lehrmann, D. J., Band, A., et al. (2020). Suppressed competitive exclusion enabled the proliferation of Permian/Triassic boundary microbialites. *Depos. Rec.* 6, 62–74. doi: 10.1002/dep2.97

Foster, W. J., Lehrmann, D. J., Yu, M. Y., and Martindale, R. C. (2019). Facies selectivity of benthic invertebrates in a Permian/Triassic boundary microbialite succession: implications for the "microbialite refuge" hypothesis. *Geobiology* 17, 523–535. doi: 10.1111/gbi.12343

Fraiser, M. L., Twitchett, R. J., and Bottjer, D. J. (2005). Unique microgastropod biofacies in the Early Triassic: indicator of long-term biotic stress and the pattern of biotic recovery after the end-Permian mass extinction. *C. R. Palevol.* 4, 543–552. doi: 10.1016/j.crpv.2005.04.006

Gliwa, J., Forel, M. B., Crasquin, S., Ghaderi, A., and Korn, D. (2021). Ostracods from the end-Permian mass extinction in the Aras Valley section (north-west Iran). *Pap. Palaeontol.* 7, 1003–1042. doi: 10.1002/spp2.1330

Hammer, Ø., Harper, D., and Ryan, P. (2001). Past: paleontological statistics software package for education and data analysis. *Palaeontol. Electron.* 4, 1–9.

Jablonski, D. (1994). Extinctions in the fossil record. *Phil. Trans. R. Soc. Lond. B.* 344, 11–17. doi: 10.1098/rstb.1994.0045

Jiang, H. S., Lai, X. L., Sun, Y. D., Wignall, P. B., Liu, J. B., and Yan, C. B. (2014). Permian-Triassic conodonts from Dajiang (Guizhou, South China) and their implication for the age of microbialite deposition in the aftermath of the End-Permian mass extinction. *J. Earth Sci.* 25, 413–430. doi: 10.1007/s12583-014-0444-4

Jost, L., Chao, A., and Chazdon, R. L. (2011). "Compositional similarity and β (beta) diversity" in *Biological Diversity: Frontiers in Measurement and Assessment*. eds. A. E. Margurran and B. J. McGill (Cambridge: Oxford University Press), 66–84.

Kershaw, S., Crasquin, S., Li, Y., Collin, P. Y., Forel, M. B., Mu, X., et al. (2012). Microbialites and global environmental change across the Permian-Triassic boundary: a synthesis. *Geobiology* 10, 25–47. doi: 10.1111/j.1472-4669.2011.00302.x

Kershaw, S., Li, Y., Crasquin, S., Feng, Q. L., Mu, X. N., Collin, P. Y., et al. (2007). Earliest Triassic microbialites in the South China block and other areas: controls on their growth and distribution. *Facies* 53, 409–425. doi: 10.1007/s10347-007-0105-5

Lehrmann, D. J., Wei, J. Y., and Enos, P. (1998). Controls on facies architecture of a large Triassic carbonate platform: the Great Bank of Guizhou, Nanpanjiang Basin, South China. *J. Sediment. Res.* 68, 311–326. doi: 10.2110/jsr.68.311

Liu, H., Wang, Y. B., Yuan, A. H., Yang, H., Song, H. J., and Zhang, S. X. (2010). Ostracod fauna across the Permian-Triassic boundary at Chongyang, Hubei Province,and its implication for the process of the mass extinction. *Sci. China Earth Sci.* 53, 810–817. doi: 10.1007/s11430-010-0045-8

Qiu, X. C., Tian, L., Wu, K., Benton, M. J., Sun, D. Y., Yang, H., et al. (2019). Diverse earliest Triassic ostracod fauna of the non-microbialite-bearing shallow marine carbonates of the Yangou section, South China. *Lethaia* 52, 583–596. doi: 10.1111/let.12332

Shen, S. Z., Crowley, J. L., Wang, Y., Bowring, S. A., Erwin, D. H., Sadler, P. M., et al. (2011). Calibrating the end-Permian mass extinction. *Science* 334, 1367–1372. doi: 10.1126/science.1213454

Shen, S. Z., Zhang, H., Zhang, Y. C., Yuan, D. X., Chen, B., He, W. H., et al. (2019). Permian integrative stratigraphy and timescale of China. *Sci. China Earth Sci.* 62, 154–188. doi: 10.1007/s11430-017-9228-4

Song, H. J., Wignall, P. B., Chu, D. L., Tong, J. N., Sun, Y. D., Song, H. Y., et al. (2014). Anoxia/high temperature double whammy during the Permian-Triassic marine crisis and its aftermath. *Sci. Rep.* 4:4132. doi: 10.1038/srep04132

Song, H. J., Wignall, P. B., Tong, J. N., and Yin, H. F. (2013). Two pulses of extinction during the Permian-Triassic crisis. *Nat. Geosci.* 6, 52–56. doi: 10.1038/ngeo1649

Sørenson, T. (1948). A method of establishing groups of equal amplitude in plant sociology based on similarity of species content. *Bull. Soc. Plant Eco.* 5, 1–34. doi: 10.18960/bse.1.1_56_1

Suárez-Mozo, N. Y., Vidal-Martínez, V. M., Aguirre-Macedo, M. L., Pech, D., Guerra-Castro, E., and Simões, N. (2021). Bivalve diversity on the continental shelf and deep sea of the Perdido Fold Belt, Northwest Gulf of Mexico, Mexico. *Diversity* 13:166. doi: 10.3390/d13040166

Tian, L., Tong, J. N., Xiao, Y. F., Benton, M. J., Song, H. Y., Song, H. J., et al. (2019). Environment instability prior to end-Permian mass extinction reflected in biotic and facies changes on shallow carbonate platform of the Nanpanjiang Basin (South China). *Palaeogeogr. Palaeoclimatol. Palaeoecol.* 519, 23–36. doi: 10.1016/j.palaeo.2018.05.011

Tong, J. N., and Yin, H. F. (2002). The lower Triassic of South China. *J. Asian Earth Sci.* 20, 803–815. doi: 10.1016/S1367-9120(01)00058-X

Wan, J. Y. (2021). *Response of Ostracod Assemblage from Microbialites in South China to the End-Permian Mass Extinction*. Dissertation Wuhan: China University of Geosciences.

Wan, J. Y., Yuan, A. H., Crasquin, S., Jiang, H. S., Yang, H., and Hu, X. (2019). High-resolution variation in ostracod assemblages from microbialites near the Permian-Triassic boundary at Zuodeng, Guangxi region, South China. *Palaeogeogr. Palaeoclimatol. Palaeoecol.* 535:109349. doi: 10.1016/j.palaeo.2019.1093349

Wang, Y. B., Tong, J. N., Wang, J. S., and Zhou, X. G. (2005). Calcimicrobialite after end-Permian mass extinction in South China and its palaeoenvironmental significance. *Chin. Sci. Bull.* 50, 665–671. doi: 10.1360/982004-323

Wang, L., Wignall, P. B., Wang, Y. B., Jiang, H. S., Sun, Y. D., Li, G. S., et al. (2016). Depositional conditions and revised age of the Permo-Triassic microbialites at Gaohua section, Cili County (Hunan Province, South China). *Palaeogeogr. Palaeoclimatol. Palaeoecol.* 443, 156–166. doi: 10.1016/j.palaeo.2015.11.032

Xiao, Y. F., Wu, K., Tian, L., Benton, M. J., Du, Y., Yang, H., et al. (2018). Framboidal pyrite evidence for persistent low oxygen levels in shallow-marine facies of the Nanpanjiang Basin during the Permian-Triassic transition. *Palaeoclimatol. Palaeoecol.* 511, 243–255. doi: 10.1016/j.palaeo.2018.08.012

Xiao, Y. F., Wang, K. Y., He, W. H., Suzuki, N., Zhang, K. X., Yang, T. L., et al. (in press). Changhsingian (Lopingian, Permian) radiolarian paleobiogeography on and around the Yangtze Platform. *Palaeoworld*. doi: 10.1016/j.palwor.2022.07.001

Yin, H. F., Jiang, H. S., Xia, W. C., Feng, Q. L., Zhang, N., and Shen, J. (2014). The end-Permian regression in South China and its implication on mass extinction. *Earth Sci. Rev.* 137, 19–33. doi: 10.1016/j.earscirev.2013.06.003

Zacaï, A., Brayard, A., Dommergues, J. L., Meister, C., Escarguel, G., Laffont, R., et al. (2016). Gauging scale effects and biogeographical signals in similarity distance decay analyses: an early Jurassic ammonite case study. *Palaeontology* 59, 671–687. doi: 10.1111/pala.12250

Zhang, S. H., Shen, S. Z., and Erwin, D. H. (2022). Two cosmopolitanism events driven by different extreme paleclimate regimes. *Glob. Planet Change* 216:103899. doi: 10.1016/j.gloplacha.2022.103899